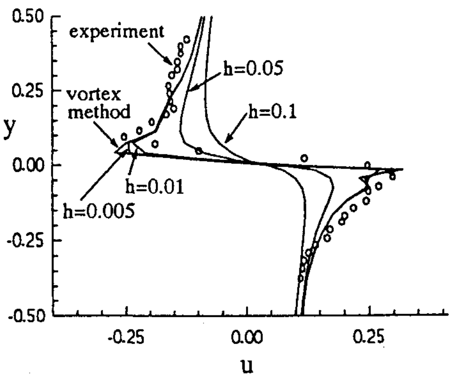

Fig. 4 For grids of different size, the computed streamwise velocity profiles across a relatively isolated vortex core are compared with the experimental result.[7]

size. When only one point vortex is distributed over the elements by the distribution scheme as shown in Fig. 1b, the numerical diffusion (error) will be introduced. But for a cluster of point vortices occupying a finite area, this error can be minimized if the grid size is small enough so that the resulting vortical patches, overlapping each other, occupy about the same region as the cluster does. In Fig. 4, the velocity profiles across a relatively isolated vortex core generated by a pitching airfoil are compared. A cluster of point vortices is generated by using the vortex panel method,[6] and, across it, the calculated velocity profile agrees well with the experimental result of Straus et al.[7] By the distribution scheme, the point vortices in the cluster are then distributed on the uniform grids of different size ($\Delta x = \Delta y = h$ and $h = 0.1$, 0.05, 0.01, and 0.005). For a finer grid size ($h \leq 0.01$), the velocity profiles obtained by the distribution scheme agree well with the experimental result[7] as shown in Fig. 4. In the numerical example presented in this section, the passing vortex is turned into a vortical patch by the distribution scheme in the vicinity of the stationary airfoil, where the grid size is less than 0.01, to ensure the accurate and smooth transition.

Summary

In this work, the distribution scheme is used to model the passing vortex as a continuous, viscous vortical patch, and the total flow including the passing vortex is governed by the Navier–Stokes equations. When the distribution scheme is applied to a cluster of point vortices on a fine-enough grid, the introduced numerical error can be minimized. The numerical results show that the effect of viscous diffusion of the passing vortex only manifests its importance on the blade–vortex interaction near the stationary airfoil.

References

[1]Wu, J. C., Hsu, T. M., Tang, W., and Sankar, L. N., "Viscous Flow Results for the Vortex-Airfoil Interaction Problem," AIAA Paper 85-4053, Oct. 1985.

[2]Hsu, T.-M., and Wu, J. C., "Theoretical and Numerical Studies of a Vortex-Airfoil Interaction Problem," AIAA Paper 86-1094, May 1986.

[3]Sarpkaya, T., "Computational Methods with Vortices—The 1988 Freeman Scholar Lecture," *Journal of Fluids Engineering*, Vol. 111, March 1989, pp. 5–51.

[4]Wu, J. C., "Numerical Boundary Conditions for Viscous Flow Problems," *AIAA Journal*, Vol. 14, No. 8, 1976, pp. 1042–1049.

[5]Baker, A. J., "Finite Element Computational Fluid Mechanics," Hemisphere, New York, 1983, pp. 101–103.

[6]Mook, D. T., and Dong, B., "Perspective: Numerical Simulations of Wakes and Blade-Vortex Interaction," *Journal of Fluids Engineering*, Vol. 116, No. 1, 1994, pp. 5–21.

[7]Straus, J., Renzoni, P., and Mayle, R. E., "Airfoil Measurements During a Blade Vortex Interaction and Comparison with Theory," *AIAA Journal*, Vol. 28, No. 2, 1990, pp. 222–228.

Mathematical Simulation of Near-Vertical Flight of Fixed-Wing Aircraft

Johan Ernest Mebius*
Delft University of Technology, 2600 Delft, The Netherlands

Nomenclature

$OXYZ$	= Earth-fixed coordinate system
$oxyz$	= body axes coordinate system
p, q, r	= body axes components of angular velocity vector
p_n, p_z	= tangent planes to S at N and Z, respectively
S, N, Z	= fictitious sphere having its center at the aircraft's c.g., and its nadir and zenith poles
$SO(3)$	= set of all three-dimensional attitudes; set of all three-dimensional rotations about a fixed point
δ	= $\psi - \phi$
λ_n, μ_n, σ	= nadir coordinates
λ_z, μ_z, δ	= zenith coordinates
σ	= $\psi + \phi$
ψ, θ, ϕ	= Euler angles of rotation from Earth-fixed to body axes coordinate system

Introduction

IN the mathematics of flight simulation two methods are commonly used to represent the aircraft attitude, the one based on Euler angles, the other based on Euler parameters and the accompanying quaternion calculus.

Euler angles have an immediate intuitive appeal and are perfectly adequate for simulations in which one stays well clear of vertical attitudes. The singularities occurring in vertical aircraft attitudes constitute a major drawback of Euler angles, which makes them unsuitable for military flight simulation and for the analysis of flight incidents and accidents in which loss of control is a major factor.

Existing software for civil flight simulation employs Euler angles. An upgrade of this software to cover out-of-control situations and other situations with arbitrarily steep pitches may be done by replacing Euler angles with Euler parameters, but doing so requires a virtually system-wide reconstruction of the software.

This Note presents a mathematical method of eliminating in turn the singularity at vertical nose-down attitudes and the singularity at vertical nose-up attitudes (simply denoted as nose-down and nose-up, respectively). This method involves the introduction of a pair of new coordinate systems for aircraft attitudes, both of them based directly on Euler angles. The one system has a singularity only at nose-up attitudes; in this Note it is denoted as the nadir system; the other only at nose-down attitudes; this is called the zenith system. For the entire method the term extended Euler angles system is proposed.

One may employ a combination of the traditional Euler angles system and the nadir and zenith coordinate systems; with an appropriate switching scheme one avoids all singularities. Flight simulation software systems thus constructed would be more complex than systems based on Euler parameters, but it is expected that the introduction of the extended Euler angles system is far easier, both from a mathematical and a software engineering viewpoint, than a conversion to Euler parameters.

Received Jan. 21, 1995; revision received Dec. 15, 1995; accepted for publication Jan. 2, 1996.

*Assistant Professor, Department of Technical Mathematics and Informatics, P.O. Box 356. e-mail: j.e.mebius@twi.tudelft.nl.

Cartesian Coordinate Systems

Two Cartesian coordinate systems are used, defined next in accordance with the conventions of aerospace mathematics.

The Earth-fixed coordinate system (ECS) has its $+X$ axis pointing to the North, its $+Y$ axis to the East and, as a consequence of the right-handedness convention, its $+Z$ axis pointing vertically downward. Its origin is taken at any convenient reference point.

The body axes coordinate system (BCS) has its $+x$ axis pointing forward, its $+y$ axis to starboard, and its $+z$ axis pointing from the aircraft's ceiling to the floor. Its origin is taken at the aircraft's c.g.

The attitude or orientation of an aircraft is represented by the rotational displacement needed to move the aircraft from the standard attitude to the actual attitude. By definition, the aircraft has the standard attitude if its forward roll axis points to the North, and its starboard axis points to the East, i.e., if no rotation is needed when moving from the ECS to the BCS. In this way an identification of the set of all three-dimensional attitudes with the set of all three-dimensional rotations about a fixed point [$SO(3)$] is obtained.

Coordinate Transformations and Euler Angles

Aircraft attitudes are conventionally represented by a triple of Euler angles as follows: the rotation R producing a specified attitude starting from the standard attitude is decomposed into a rotation $R_{Z,\psi}$ from North to actual heading about the downward vertical axis (i.e., the $+Z$ axis) through ψ, followed by a rotation $R_{y,\theta}$ about the aircraft's starboard traverse axis (the $+y$ axis) through θ, which is at last followed by a rotation $R_{x,\phi}$ about the aircraft's forward roll axis (the $+x$ axis) through ϕ. According to the terminology of Ref. 1, ψ is the aircraft's heading, θ is its attitude, and ϕ is its bank; in this Note the term pitch angle is preferred to attitude because of the more general meaning of the word attitude.

The general rotation R is represented by

$$M_R = \begin{bmatrix} \cos\psi\cos\theta & -\sin\psi\cos\phi + \cos\psi\sin\theta\sin\phi & \sin\psi\sin\phi + \cos\psi\sin\theta\cos\phi \\ \sin\psi\cos\theta & \cos\psi\cos\phi + \sin\psi\sin\theta\sin\phi & -\cos\psi\sin\phi + \sin\psi\sin\theta\cos\phi \\ -\sin\theta & \cos\theta\sin\phi & \cos\theta\cos\phi \end{bmatrix} \tag{1}$$

This formula will be needed on several occasions. For its derivation the reader is referred to the existing literature.[1-3]

Euler Angle Singularities and Vertical Attitudes

Very well known are the singularities, because for $\theta = \pm\pi/2$, the undirected roll axis is vertical and therefore coincides with the undirected yaw axis in its initial position. This situation somewhat resembles the gimbal lock phenomenon of a gyroscope when the gimbals are in such an orientation that the precession and spin axes coincide. While the gimbal lock is a mechanical phenomenon, the Euler angle singularities are of a purely mathematical nature and have nothing to do with flight mechanics per se. Less well known seems the fact that whereas both ψ and ϕ are indeterminate for nose-down as well as for nose-up attitudes, the sum $\sigma = \psi + \phi$ remains well determined for nose-down attitudes, and furthermore, completely determines the attitude in that case. Analogously, the difference $\delta = \psi - \phi$ remains well determined for nose-up attitudes and completely determines the attitude in that case.

Consider, for instance, nose-down attitudes. The attitude ($\psi = 0$, $\theta = -\pi/2$, $\phi = 0$) may be considered in this paragraph as a reference nose-down attitude. Consider next an arbitrary nose-down attitude (ψ, $-\pi/2$, ϕ). It may be obtained from the reference nose-down attitude by a rotation through $\psi + \phi$ about the positive vertical axis. Now forget the specific values of ψ and ϕ. Because the positive roll axis coincides with the positive vertical axis, one can no longer tell what part of the total rotation was because of the initial yaw (i.e., turning from North to actual heading) and what part to the final roll (i.e., rolling from level to bank). An analogous observation applies to nose-up attitudes.

Straightforward algebraic proof is furnished by the substitution of θ by $\pm\pi/2$ in Eq. (1). The conclusion is that σ is indeterminate only for $\theta = \pi/2$, and δ only for $\theta = -\pi/2$.

Equations of Motion of a Rigid Aircraft

Equations of motion of a single rigid body are mostly solved numerically as an initial-value problem by some method of stepwise integration with respect to time. The two main steps in each integration cycle are 1) the calculation of the next values of the linear and angular velocities from their previous values and the force and moment components (and the mass and the moments and products of inertia, of course) and 2) the calculation of the next values of the position and attitude coordinates from their previous values and the linear and angular velocity components.

Dynamics

Step 1: the integration of accelerations into velocities, essentially reflects the entire dynamics of the motion problem. It is based on Newton's equations of translational motion of the c.g. and Euler's equations of rotational motion of a rigid body about its c.g. No need to list them here; the reader is referred to the existing literature.

The integration of accelerations into velocities does not involve singularities beyond those that may be present in the force and moment components.

Kinematics

Step 2: consisting of the integration of linear velocities into position coordinates and of angular velocities into attitude coordinates, is on the other hand a purely kinematical operation.

Translational Kinematics

The position is obtained by integration of the equations that express the ECS components of the linear velocity in terms of the BCS components. The reader is again referred to the existing literature.

Rotational Kinematics

Obtaining the attitude coordinates from the angular velocity components is more difficult because one cannot parametrize the entire $SO(3)$ with three coordinates without incurring singularities. Essentially this is because of topological properties of $SO(3)$ following from its curved nature.

The angular velocity components expressed in terms of Euler rates are

$$\begin{aligned} p &= -\dot\psi\sin\theta + \dot\phi \\ q &= \dot\psi\cos\theta\sin\phi + \dot\theta\cos\phi \\ r &= \dot\psi\cos\theta\cos\phi - \dot\theta\sin\phi \end{aligned} \tag{2}$$

the Euler rates expressed in terms of angular velocity are

$$\dot\psi = (q\sin\phi + r\cos\phi)\sec\theta \tag{3}$$

$$\dot\theta = q\cos\phi - r\sin\phi \tag{4}$$

$$\dot\phi = p + (q\sin\phi + r\cos\phi)\tan\theta \tag{5}$$

The change rates of σ and δ in terms of p, q, r are

$$\dot{\sigma} = p + (q \sin \phi + r \cos \phi)\tan(\theta/2 + \pi/4) \quad (6)$$

$$\dot{\delta} = -p + (q \sin \phi + r \cos \phi)\cot(\theta/2 + \pi/4) \quad (7)$$

The last two expressions are obtained by addition and subtraction of Eqs. (3) and (5), using the identities

$$\sec \theta \pm \tan \theta \equiv (1 \pm \sin \theta)/\cos \theta$$

$$\equiv \tan(\pi/4 \pm \theta/2) \equiv \cot(\pi/4 \mp \theta/2)$$

Coordinate Systems for Near-Vertical Attitudes

In this section the previously mentioned nadir and zenith coordinate systems are introduced. They are best understood by building a geometrical representation of the aircraft's attitude.

Geometrical Representation

Imagine the aircraft at the center of a sphere S of unit diameter flying together with the aircraft (Fig. 1). The aircraft's forward roll axis intersects S in some point A. The heading ψ and pitch angle θ of the aircraft are the longitude and latitude coordinates of A on S. Instead of ψ and θ to represent the direction of the forward roll axis, the point A itself may be taken.

To account for the rolling displacement, the point A is provided with a vector $\boldsymbol{u}$ of arbitrary fixed length l representing the direction of the starboard wing (in Fig. 1 represented by a great-circle segment on S). The combination $(A, \boldsymbol{u})$ in Fig. 1 faithfully and completely represents the aircraft's attitude and may be viewed as an aircraft attitude symbol.

The set of all possible starboard wing directions at A may be imagined as a disc (not shown in Fig. 1) consisting of all tangent vectors to S at A of length l. In this way the attitude space $SO(3)$ looks like a spherical surface decorated everywhere with discs of uniform radius l.

The next step is to perform a stereographic projection of S from its zenith pole Z onto the tangent plane p_n at the nadir pole N. The stereographic projection is restricted to spheres and planes, but otherwise it is an ordinary central projection. It is a conformal mapping, i.e., angles between intersecting smooth curves within S are preserved under projection.

Consider the projection of S from Z onto p_n. All of S, except the single point Z, is mapped onto p_n. Again observe Fig. 1. The stereographic projection maps points to points; specifically it maps A on S to A_n in p_n. But A was provided with a vector $\boldsymbol{u}$. The $\boldsymbol{u}$ is mapped onto a line segment u_n in p_n (u_n is represented in Fig. 1 by a circular arc). Because of the conformal property the position angle ϕ of $\boldsymbol{u}$ in its disc at A will be projected unaltered into p_n. One may say that stereographic projection maps the combination $(A, \boldsymbol{u})$ to the combination (A_n, u_n).

Now observe A_n and u_n. The former represents a two-dimensional translation in p_n from N to A_n, the latter represents a two-dimensional rotation in p_n about A_n through the angle $\psi + \phi$; this rotation is taken with respect to a reference position of vectors in p_n at A_n defined by $\psi + \phi = 0$. It reflects the combined effects of turning from North to actual heading and rolling from level to bank.

Therefore, the stereographic zenith-to-nadir projection establishes a singularity-free one-to-one mapping between the set of all attitudes different from nose-up on the one hand and all two-dimensional displacements in the plane p_n on the other hand. Finally, a two-dimensional displacement in p_n is parametrized by the N–S and E–W components of the translation and the angle of the subsequent rotation. These three displacement parameters constitute the nadir coordinates of the attitude.

By interchanging the roles of nadir and zenith in the previous reasoning, one obtains zenith coordinates, defined in the

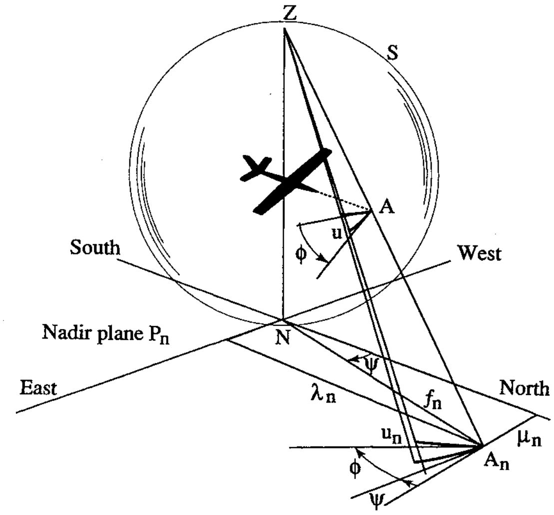

Fig. 1 Stereographic projection for the nadir coordinate system (attitude ψ = 15 deg, θ = 0 deg, ϕ = 35 deg).

plane p_z (not shown in Fig. 1) and valid for all attitudes different from nose-down.

Nadir Coordinates

Based on the geometrical picture of the previous section, the nadir coordinates λ_n, μ_n, σ are defined in terms of the Euler angles as follows:

$$\lambda_n = f_n \cos \psi, \qquad \mu_n = f_n \sin \psi, \qquad \sigma = \psi + \phi \quad (8)$$

where

$$f_n = \tan(\theta/2 + \pi/4) \quad (9)$$

It is convenient to define rotated Cartesian coordinates in p_n as follows:

$$\zeta_n = f_n \cos \phi, \qquad \eta_n = f_n \sin \phi \quad (10)$$

Remark that $\lambda_n^2 + \mu_n^2 = \zeta_n^2 + \eta_n^2 = f_n^2$.

Straightforward calculations yield the three-dimensional rotation matrix (1) in terms of the nadir coordinates:

$$a_{11} = \cos \psi \cos \theta$$
$$= 2\lambda_n/D_n$$
$$a_{12} = -\sin \psi \cos \phi + \cos \psi \sin \theta \sin \phi$$
$$= (-1 + 2\lambda_n^2/D_n)\sin \sigma - (2\lambda_n\mu_n/D_n)\cos \sigma$$
$$a_{13} = \sin \psi \sin \phi + \cos \psi \sin \theta \cos \phi$$
$$= (-1 + 2\lambda_n^2/D_n)\cos \sigma + (2\lambda_n\mu_n/D_n)\sin \sigma$$
$$a_{21} = \sin \psi \cos \theta$$
$$= 2\mu_n/D_n$$
$$a_{22} = \cos \psi \cos \phi + \sin \psi \sin \theta \sin \phi$$
$$= (1 - 2\mu_n^2/D_n)\cos \sigma + (2\lambda_n\mu_n/D_n)\sin \sigma$$
$$a_{23} = -\cos \psi \sin \phi + \sin \psi \sin \theta \cos \phi$$
$$= (-1 + 2\mu_n^2/D_n)\sin \sigma + (2\lambda_n\mu_n/D_n)\cos \sigma$$
$$a_{31} = -\sin \theta$$
$$= (1 - f_n^2)/D_n$$
$$a_{32} = \cos \theta \sin \phi$$
$$= 2(\lambda_n \sin \sigma - \mu_n \cos \sigma)/D_n$$

$$a_{33} = \cos\theta\cos\phi = 2(\lambda_n\cos\sigma + \mu_n\sin\sigma)/D_n$$

where $D_n = 1 + f_n^2 = 1 + \lambda_n^2 + \mu_n^2$.

Differentiation of Eqs. (8) to t yields [using Eqs. (4), (3), the identity $1 + f_n^2 \equiv 2f_n \sec\theta$ and Eq. (6)]:

$$\dot f_n = D_n\dot\theta/2 \tag{11}$$

$$\dot\lambda_n = D_n(q\cos\sigma - r\sin\sigma)/2, \quad \dot\mu_n = D_n(q\sin\sigma + r\cos\sigma)/2 \tag{12}$$

$$\dot\sigma = p + q\eta_n + r\zeta_n = p + q(\lambda_n\sin\sigma - \mu_n\cos\sigma) + r(\lambda_n\cos\sigma + \mu_n\sin\sigma) \tag{13}$$

where again, $D_n = 1 + f_n^2 = 1 + \lambda_n^2 + \mu_n^2$.

Zenith Coordinates

In analogy with the preceding subsection the zenith coordinates λ_z, μ_z, δ are defined in terms of the Euler angles as follows:

$$\lambda_z = f_z\cos\psi, \qquad \mu_z = f_z\sin\psi, \qquad \delta = \psi - \phi \tag{14}$$

where

$$f_z = \tan(-\theta/2 + \pi/4) \tag{15}$$

The rotated Cartesian coordinates are

$$\zeta_z = f_z\cos\phi, \qquad \eta_z = f_z\sin\phi \tag{16}$$

Remark that $\lambda_z^2 + \mu_z^2 = \zeta_z^2 + \eta_z^2 = f_z^2$.

Straightforward calculations yield the three-dimensional rotation matrix (1) in terms of the zenith coordinates:

$$a_{11} = \cos\psi\cos\theta = 2\lambda_z/D_z$$

$$a_{12} = -\sin\psi\cos\phi + \cos\psi\sin\theta\sin\phi = (-1 + 2\lambda_z^2/D_z)\sin\delta - (2\lambda_z\mu_z/D_z)\cos\delta$$

$$a_{13} = \sin\psi\sin\phi + \cos\psi\sin\theta\cos\phi = (1 - 2\lambda_z^2/D_z)\cos\delta - (2\lambda_z\mu_z/D_z)\sin\delta$$

$$a_{21} = \sin\psi\cos\theta = 2\mu_z/D_z$$

$$a_{22} = \cos\psi\cos\phi + \sin\psi\sin\theta\sin\phi = (1 - 2\mu_z^2/D_z)\cos\delta + (2\lambda_z\mu_z/D_z)\sin\delta$$

$$a_{23} = -\cos\psi\sin\phi + \sin\psi\sin\theta\cos\phi = (1 - 2\mu_z^2/D_z)\sin\delta - (2\lambda_z\mu_z/D_z)\cos\delta$$

$$a_{31} = -\sin\theta = (-1 + f_z^2)/D_z$$

$$a_{32} = \cos\theta\sin\phi = 2(-\lambda_z\sin\delta + \mu_z\cos\delta)/D_z$$

$$a_{33} = \cos\theta\cos\phi = 2(\lambda_z\cos\delta + \mu_z\sin\delta)/D_z$$

where $D_z = 1 + f_z^2 = 1 + \lambda_z^2 + \mu_z^2$.

Differentiation of Eqs. (14) to t yields [using Eqs. (4), (3), the identity $1 + f_z^2 \equiv -2f_z\sec\theta$, and Eq. (7)]:

$$\dot f_z = -D_z\dot\theta/2 \tag{17}$$

$$\dot\lambda_z = -D_z(q\cos\delta + r\sin\delta)/2, \qquad \dot\mu_z = -D_z(q\sin\delta - r\cos\delta)/2 \tag{18}$$

$$\dot\delta = -p + q\eta_z + r\zeta_z = -p + q(-\lambda_z\sin\delta + \mu_z\cos\delta) + r(\lambda_z\cos\delta + \mu_z\sin\delta) \tag{19}$$

where again, $D_z = 1 + f_z^2 = 1 + \lambda_z^2 + \mu_z^2$.

The external forces and moments are in general functions of, among other quantities, ψ, θ, and ϕ. But as long as the external forces and moments do not happen to be singular for vertical attitudes, one can be sure to obtain well-behaved expressions for the external forces and moments upon replacement of ψ, θ, ϕ with λ_n, μ_n, σ or λ_z, μ_z, δ.

Switching Among Attitude Coordinate Systems

From numerical analysis it is known that absolute errors in functional relations are propagated with a factor equal to the magnitude of the derivative.

With the help of the formulas $d(\tan\theta)/d\theta = \sec^2\theta$ and $d(\sec\theta)/d\theta = \tan\theta\sec\theta$, it is found that in Eqs. (3) and (5) one suffers one decimal place of significance loss at $|\theta| \approx 72$ deg and two at $|\theta| \approx 84$ deg.

Dependent upon the acceptable significance loss a threshold value $\Theta > 0$ is selected and three flight regimes are established. The normal regime, defined by $-\Theta \le \theta \le \Theta$, is covered by the traditional Euler angles system; the nose-up regime, defined by $\theta \ge \Theta$, is covered by the zenith coordinate system; the nose-down regime, defined by $\theta \le -\Theta$, is covered by the nadir coordinate system.

Switching among the three systems occurs once in a while, and the computing time involved is expected to fit into available time slices of simulation runs; in a simulation program running on personal computers no glitches were observed when switching.

In theory, it suffices to employ only the zenith and nadir coordinate systems and to establish only two flight regimes, namely a nose-up regime for the entire upper hemisphere and extending way down to the nadir ($-\Theta \le \theta \le \frac{1}{2}\pi$), and a nose-down regime for the entire lower hemisphere and extending way up to the zenith ($-\frac{1}{2}\pi \le \theta \le \Theta$). They overlap along the zone $-\Theta \le \theta \le \Theta$, the previously mentioned normal regime.

In this setup, one switches to zenith (nadir) coordinates when an increasing (decreasing) pitch angle θ passes the $\Theta(-\Theta)$ boundary, if not already in zenith (nadir) mode. When flying in the normal regime one is in the zenith or nadir mode, depending upon motion history. However, when doing so one has to deal with a nonuniform integration error behavior in time, which is moreover not symmetrical with respect to level flight. Therefore the setup with three flight regimes is preferred.

Acknowledgments

The author thanks M. Baarspul, H. Koppelaar, C. A. A. M. van der Linden, J. A. Mulder, and T. H. M. Smits for their careful reading and suggestions for improvement, and J. Schonewille for the artwork.

References

[1]Anon., "Dynamics of Flight: An Intensive Course for Practicing Engineers," Univ. of Michigan, Ann Arbor, MI, Aug. 1958.

[2]Baarspul, M., "A Review of Flight Simulation Techniques," *Progress in Aerospace Sciences*, Vol. 27, Pergamon, Oxford, England, UK, 1990, pp. 1–120.

[3]Rolfe, J. M., and Staples, K. J. (eds.), "Flight Simulation," *Cambridge Aerospace Series*, Cambridge Univ. Press, Cambridge, England, UK, 1986.